Eur. Phys. J. B **39**, 249–260 (2004)
DOI: 10.1140/epjb/e2004-00188-7

THE EUROPEAN PHYSICAL JOURNAL B

Microscopic theory of equilibrium properties of F/S/F trilayers with weak ferromagnets

R. Mélin[a]

Centre de Recherches sur les Très Basses Températures (CRTBT)[b], B.P. 166, 38042 Grenoble Cedex 9, France

Received 23 January 2004
Published online 29 June 2004 –

Abstract. The aim of this paper is to explain the non monotonic temperature dependence of the self-consistent superconducting gap of ferromagnet/superconductor/ferromagnet (F/S/F) trilayers with weak ferromagnets in the parallel alignment (equivalent to F/S bilayers). We show that this is due to Andreev bound states that compete with the formation of a minigap. Using a recursive algorithm we discuss in detail the roles of various parameters (thicknesses of the superconductor and ferromagnets, relative spin orientation of the ferromagnets, exchange field, temperature, disorder, interface transparencies).

PACS. 74.78.Na Mesoscopic and nanoscale systems – 74.45.+c Proximity effects; Andreev effect; SN and SNS junctions – 74.50.+r Tunneling phenomena; point contacts, weak links, Josephson effects

1 Introduction

In conventional superconductivity the attractive interaction mediated by phonons binds electrons into Cooper pairs that condense in the BCS ground state with a zero temperature gap Δ to the first quasiparticle excitations [1]. In ferromagnetism electron interactions generate a spin symmetry breaking that can be described by the Stoner model in which electrons subject to an exchange field $h_{\rm ex}$ acquire a Zeeman energy.

Many physical phenomena are involved at the interfaces between superconductors (Ss) and ferromagnets (Fs). For instance it was shown in the early 1970's that the Fermi surface spin polarization of a ferromagnetic metal could be measured by spin-resolved tunneling between a ferromagnet and a superconducting film in the presence of Zeeman splitting [2]. The Fermi surface spin polarization was measured more recently [3,4] by Andreev reflection at F/S interfaces [5] with highly transparent interfaces, not in thin film geometries. The non equilibrium spin population in the ferromagnet plays also a role in Andreev reflection at F/S interfaces [6–8]. Andreev reflection with Zeeman splitting in a thin film geometry could be another way to probe the Fermi surface spin polarization [9].

These experiments can be interpreted without discussing the proximity effect (the pair correlations induced in the normal metal or ferromagnet) that has focused an important interest recently. It is well established both theoretically and experimentally that the pair amplitude induced in a ferromagnetic metal oscillates in space and can become negative [10–14], giving rise to the π-coupling. The π-coupling generates oscillations of the critical temperature of F/S multilayers as a function of the thickness of the ferromagnetic layers [15–19]. The bad quality of interfaces may however also play a role in these experiments [20,21]. Direct evidences of the π-coupling have been obtained recently [22–25]. The proximity effect at F/S interfaces is related to the formation of the so-called Andreev bound states. Andreev bound states were first discussed by de Gennes and Saint-James [26] and Andreev [27] for normal metal (N)/S interfaces. Several theoretical investigations of Andreev bound states at F/S interfaces have been presented recently [21,28,29] as well as numerical investigations of the proximity effect at F/S interfaces, based on simulations of the Bogoliubov-de Gennes equations [30].

The interest in the inverse proximity effect (the properties of the superconductor) at F/S interfaces dates back to the 1960's [31–33] where it was shown that with insulating ferromagnets an exchange field is induced in the superconducting electrode of a F/S/F trilayer in the parallel alignment. The theoretical prediction by de Gennes [31] was further confirmed by experiments in the late 1960's with metallic [32] and insulating [33] ferromagnets. Recent experiments were carried out with metallic ferromagnets, which confirmed the effect on the critical temperature [34]. It was shown recently [36,35] that an exchange field in the superconductor exists also with metallic ferromagnets but the sign of the magnetization in the superconductor is opposite to the magnetization in the ferromagnet. An exchange field in a superconductor is pair breaking. As a consequence the superconducting transition temperature

[a] e-mail: melin@grenoble.cnrs.fr
[b] U.P.R. 5001 du CNRS, Laboratoire conventionné avec l'Université Joseph Fourier

in the parallel alignment is smaller than in the antiparallel alignment.

With metallic ferromagnets the proximity effect may influence the value of the superconducting gap and transition temperature. It was realized recently [36–40] that the proximity effect in F/S/F trilayers is quite special since under some conditions the zero temperature superconducting gap in the parallel alignment can be larger than in the antiparallel alignment. This was established [36,37] within a model of multiterminal hybrid structure originally proposed for transport properties [41–45] and is related to spatially separated superconducting correlations among the two ferromagnets. The same behavior was found within a model of F/S/F trilayer with atomic thickness and half-metal ferromagnets [39], which was finally extended to Stoner ferromagnets [40].

Other physical effects take place with weak ferromagnets for which the exchange field is smaller than the superconducting gap, as indicated by the reentrance of the critical temperature of F/S superlattices as a function of the exchange field [46,47], and by the reentrance of the critical temperature of F/S bilayers as a function of the thickness of the ferromagnet [38,48,49]. The full temperature dependence of the self-consistent superconducting gap was calculated in reference [40] and it was shown that for F/S bilayers or F/S/F trilayers with atomic thickness the superconducting gap can have a non monotonic temperature dependence: within a given range of parameters the superconducting gap first increases as temperature T is reduced, reaches a maximum, and decreases to zero as T is further reduced. Within a narrow range of interface transparencies there exists also a reentrant behavior of the superconducting gap at low temperature [40].

The purpose of this article is to show that this behavior is related to the formation of Andreev bound states that can compete with the formation of a superconducting minigap. We find a systematic correlation between Andreev bound states at the Fermi level and a reduction of the low temperature self-consistent superconducting gap, which constitutes the main result of this article.

The article is organized as follows. Preliminaries are given in Section 2 in which we discuss the models and the Green's functions formalism. A recursive algorithm, more efficient than the direct inversion of the Dyson matrix [40], is presented in Section 3. Different regimes can be obtained depending on how the lateral dimensions L_S of the superconductor and L_F of the ferromagnets compare respectively (i) to the zero temperature lateral superconducting coherence length $\xi_S^{(\perp)} = 2t_0a_0/\pi\Delta$ [28], where t_0 is the lateral hoping amplitude, and a_0 is equal to the interatomic distance in the transverse direction; and (ii) to the zero temperature lateral exchange length $\xi_F^{(\perp)} = 2t_0a_0/\pi h_{\rm ex}$ [28]. We present a detailed investigation of the different regimes $L_F, L_S \ll \xi_S^{(\perp)}$ (Sect. 4); $L_S \lesssim \xi_S^{(\perp)}$ and $L_F \ll \xi_F^{(\perp)}$ (Sect. 5); $L_S \ll \xi_S^{(\perp)}$ and $L_F \gtrsim \xi_F^{(\perp)}$ (Sect. 6). We cannot carry out a systematic study of the regime $L_S \sim \xi_S^{(\perp)}$, $L_F \gtrsim \xi_F^{(\perp)}$ which is too demanding from a computational point of view. In Section 7 we provide a comparison with other models proposed recently to describe Andreev bound states in F/S hybrids [28,29]. Concluding remarks are given in Section 8.

2 Preliminaries

2.1 The models

We suppose that the two ferromagnets of the F/S/F trilayer have the same thickness L_F. We note L_S the thickness of the superconductor (see Fig. 1). The three electrodes are made of 2D planes stacked along the z axis (see Fig. 2). Each superconducting plane is described by the BCS Hamiltonian

$$\mathcal{H}_{\rm BCS}^{(2D)} = \sum_{\mathbf{k},\sigma} \epsilon(k) c^+_{\mathbf{k},\sigma} c_{\mathbf{k},\sigma} + \Delta \sum_{\mathbf{k}} \left(c^+_{\mathbf{k},\uparrow} c^+_{-\mathbf{k},\downarrow} + c_{\mathbf{k},\downarrow} c_{-\mathbf{k},\uparrow} \right), \quad (1)$$

where the wave vector $\mathbf{k}$ is parallel to the 2D layer. The free electron dispersion relation within one layer is $\epsilon(k) = \hbar^2 k^2/2m$. The ferromagnets are described by the Stoner model

$$\mathcal{H}_{\rm Stoner}^{(2D)} = \sum_{\mathbf{k},\sigma} \epsilon(k) c^+_{\mathbf{k},\sigma} c_{\mathbf{k},\sigma} - h_{\rm ex} \sum_{\mathbf{k}} \left(c^+_{\mathbf{k},\uparrow} c_{\mathbf{k},\uparrow} - c^+_{\mathbf{k},\downarrow} c_{\mathbf{k},\downarrow} \right), \quad (2)$$

where $h_{\rm ex}$ is the exchange field. The coupling between two planes belonging to the same superconducting or ferromagnetic electrode is given by

$$\mathcal{W}_{\rm F-F} = \mathcal{W}_{\rm S-S} = t_0 \sum_{\mathbf{x}_L,\sigma} \left(c^+_{\mathbf{x}_L,\sigma} c_{\mathbf{x}_R,\sigma} + c^+_{\mathbf{x}_R,\sigma} c_{\mathbf{x}_L,\sigma} \right), \quad (3)$$

whereas the coupling between the ferromagnets and the superconductor is given by

$$\mathcal{W}_{\rm F-S} = t \sum_{\mathbf{x}_L,\sigma} \left(c^+_{\mathbf{x}_L,\sigma} c_{\mathbf{x}_R,\sigma} + c^+_{\mathbf{x}_R,\sigma} c_{\mathbf{x}_L,\sigma} \right), \quad (4)$$

where the summation runs over all sites at the interface ($\mathbf{x}_L$ corresponds to a site on the left side and $\mathbf{x}_R$ is the corresponding site on the right side). The parameters are such that the coherence length within one layer $\xi_S^{(\parallel)} = \hbar v_F^{(\parallel)}/\Delta$ and the transverse coherence length $\xi_S^{(\perp)} = 2t_0a_0/\pi\Delta$ are larger than the width L_S of the superconductor. The model should strictly speaking apply to ballistic systems whereas real samples are usually in the diffusive regime. However we can include disorder in one particular case (the F/S/F trilayer with atomic thickness, see Sect. 4.3).

In this case the qualitative behavior is robust against increasing disorder. Fabry-Perot resonances generate parity effects for small values of L_S and L_F in the ballistic

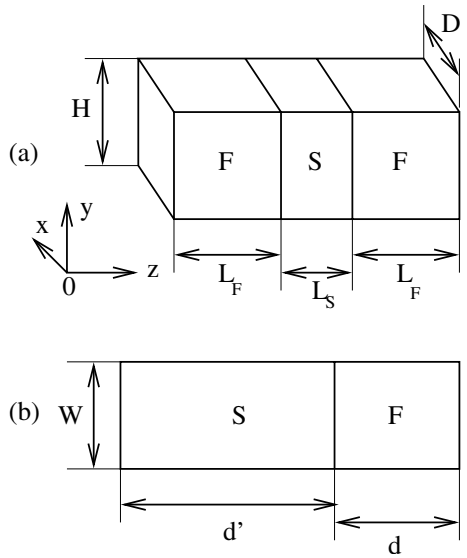

Fig. 1. (a) Schematic representation of the F/S/F trilayer. D and H are sent to to infinity (infinite planar geometry). The ferromagnets (superconductor) are made of L_F (L_S) layers stacked in the lateral (z) direction. (b) Schematic representation of the 2D F/S interface model [29] considered in Section 7.2. d' is sent to infinity.

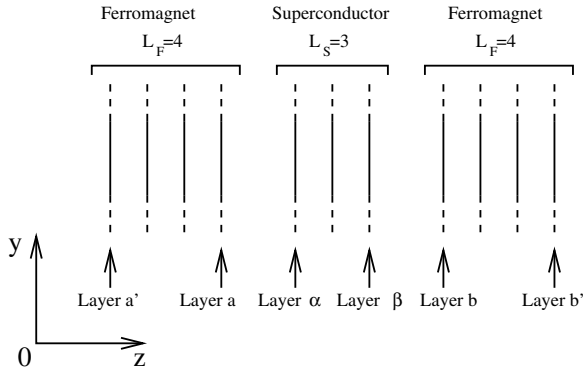

Fig. 2. Cut in the (z, y) plane of the F/S/F trilayer with $(L_S/a_0, L_F/a_0) = (3, 4)$, where a_0 is the interplane spacing. The ferromagnets and the superconductor are infinite in the x and y directions. The left ferromagnet ends at the layers a' and a. The right ferromagnet ends at the layers b and b'. The superconductor ends at layers α and β.

model. These parity effects are not expected to occur in the diffusive regime, but do not occur either in our simulations if L_S and L_F are sufficiently large. By increasing L_F and L_S we obtain a cross-over between the regime $L_F, L_S \lesssim \lambda_F$ and the regime $\lambda_F \lesssim L_F, L_S \ll \xi_S^{(\perp)}$. We find the same qualitative effects in the two regimes. Moreover we obtain in Section 5 a non monotonic variation of the self-consistent superconducting gap as a function of the exchange field. This is compatible with the non monotonic variation of the critical temperature as a function of the exchange field [38,48,49] obtained in the context of linearized Usadel equations for disordered conductors. The compatibility between the two behaviors indicates the validity of our approach.

2.2 Green's functions

2.2.1 Zero temperature Green's functions

The Green's functions of an isolated superconductor can be gathered in a 4×4 matrix in the spin $\otimes$ Nambu representation but in the absence of non collinear magnetizations [44,50–52] the quantization axis can be chosen parallel to the exchange field so that the 4×4 Green's functions reduce to two separate 2×2 matrices, one in each spin sector. For practical purpose we work in the spin-up sector. The Green's function is given by

$$\hat{g}_{\mathbf{x},\mathbf{y}}(t,t') = -i \begin{pmatrix} \left\langle T_t \left(c_{\mathbf{x},\uparrow}(t), c^+_{\mathbf{y},\uparrow}(t') \right) \right\rangle & \left\langle T_t \left(c_{\mathbf{x},\uparrow}(t), c_{\mathbf{y},\downarrow}(t') \right) \right\rangle \\ \left\langle T_t \left(c^+_{\mathbf{x},\downarrow}(t), c^+_{\mathbf{y},\uparrow}(t') \right) \right\rangle & \left\langle T_t \left(c^+_{\mathbf{x},\downarrow}(t), c_{\mathbf{y},\downarrow}(t') \right) \right\rangle \end{pmatrix}, \quad (5)$$

where $\mathbf{x}$ and $\mathbf{y}$ are two arbitrary sites in the superconductor and T_t is the usual T-product [53]. The "11" component describes the propagation of a spin-up electron, the "22" component describes the propagation of a spin-down hole and the "12" and "21" components describe superconducting correlations. After Fourier transforming we obtain a standard expression for the different elements of the Green's function [53]:

$$g^{1,1}_{\alpha,\alpha}(\xi,\omega) = \frac{u_k^2}{\omega - E_k + i\eta} + \frac{v_k^2}{\omega + E_k - i\eta} \quad (6)$$

$$f^{1,2}_{\alpha,\alpha}(\xi,\omega) = -\frac{\Delta}{[\omega - E_k + i\eta]\,[\omega + E_k - i\eta]}. \quad (7)$$

The variable ξ is related to the kinetic energy: $\xi_k = \hbar^2 k^2/(2m) - \epsilon_F$ where $\epsilon_F = \hbar^2 k_F^2/2m$ is the Fermi energy. $E_k = \sqrt{\Delta^2 + \xi_k^2}$ is the quasiparticle energy and $u_k^2 = (1 + \xi_k/E)/2$ and $v_k^2 = (1 - \xi_k/E)/2$ are the BCS coherence factors.

The Green's function of a spin-up ferromagnet is diagonal in Nambu space. The "11" component is given by

$$g^{1,1}_{a,a}(\xi,\omega) = \frac{1}{[\omega - \xi + h_{\rm ex} + i\eta\ \mathrm{sgn}(\xi - h_{\rm ex})]}, \quad (8)$$

and the Green's functions of a spin-down ferromagnet are obtained by changing $h_{\rm ex}$ into $-h_{\rm ex}$.

The Green's functions $\hat{G}_{\mathbf{x},\mathbf{y}}$ of the connected trilayer are given by the Dyson equation $\hat{G} = \hat{g} + \hat{g} \otimes \hat{\Sigma} \otimes \hat{G}$, where in a compact notation $\hat{\Sigma}$ is the self-energy corresponding to the tunnel Hamiltonian (4) and $\otimes$ corresponds to a summation over spatial variables and a convolution over time variables. We look for non perturbative solutions of the Dyson equations suitable for describing Andreev bound states.

2.2.2 Finite temperature Green's functions

Finite temperature Green's functions are obtained through the analytic continuation $\omega \to i\omega$ and by summing over the Matsubara frequencies $\omega_n = (2n+1)\pi T$

where T is the temperature [53]. The superconducting gap is determined from the BCS self-consistency equation [53]

$$\Delta_{\mathbf{x}} = \lambda T \sum_n \int \frac{d^2\mathbf{k}}{(2\pi)^2} G^{1,2}_{\mathbf{x},\mathbf{x}}(\mathbf{k}, i\omega_n), \tag{9}$$

where λ is the strength of the attractive electron-electron interaction. To evaluate (9) we change variable to $\xi = \hbar^2k^2/(2m) - \epsilon_F$ and restrict the integral to $|\xi| < \omega_D$. To avoid introducing new parameters we use $\omega_D = \epsilon_F = \hbar^2k_F^2/2m$. We note Δ_0 the superconducting gap of an isolated 2D layer. All energy scales will be compared to Δ_0.

3 Recursive algorithm for the F/S/F trilayer

3.1 Green's functions of an isolated electrode

We aim to describe F/S/F trilayers with a finite thickness of all electrodes. In this respect the $(L_S/a_0, L_F/a_0) = (1, 1)$ trilayer is just viewed as a toy-model: we use a mean field approach that does not incorporate the phase fluctuations of the order parameter and we do not consider possible instabilities such as spin or charge density wave.

The ferromagnetic and superconducting electrodes of the F/S/F trilayer consist of a finite number of layers stacked along the z axis and labeled from 1 to L (see Fig. 2). Two consecutive layers n and $n+1$ are coupled by a tunnel amplitude t_n. We use Green's functions that are parametrized by the wave vector in the (x, y) direction and by the spatial coordinate in the lateral direction.

We note $\hat{h}^{(L)}_{i,j}$ the Green's functions of the system of L layers in a given electrode and $\hat{g}_{i,i}$ the Green's function of the isolated layer number i. The Green's function $\hat{h}^{(L)}_{L,L}$ can be calculated recursively through a matrix continued fraction:

$$\hat{h}^{(L)}_{L,L} = \left[\hat{I} - \hat{g}_{L,L}\hat{t}_{L-1}\hat{h}^{(L-1)}_{L-1,L-1}\hat{t}_{L-1}\right]^{-1} \hat{g}_{L,L}. \tag{10}$$

The local Green's functions of the system of L stacked layers are obtained through

$$\hat{h}^{(L)}_{i,i} = \hat{h}^{(L-1)}_{i,i} + \hat{h}^{(L-1)}_{i,L-1}\hat{t}_{L-1}\hat{h}^{(L)}_{L,L}\hat{t}_{L-1}\hat{h}^{(L-1)}_{L-1,i}, \tag{11}$$

where $\hat{h}^{(L)}_{i,L}$ and $\hat{h}^{(L)}_{L,i}$ are calculated recursively through the relations $\hat{h}^{(L)}_{L,i} = \hat{h}^{(L)}_{L,L}\hat{t}_{L-1}\hat{h}^{(L-1)}_{L-1,i}$ and $\hat{h}^{(L)}_{i,L} = \hat{h}^{(L-1)}_{i,L-1}\hat{t}_{L-1}\hat{h}^{(L)}_{L,L}$. The computation time required to obtain $\hat{h}^{(L)}_{L,L}$ is proportional to L whereas it is proportional to L^2 if one wants to calculate all the $\hat{h}^{(L)}_{i,i}$.

3.2 Green's functions of the connected trilayer

We note $\hat{G}$ the Green's functions of the connected F/S/F trilayer (see Fig. 2). Layers a and α are connected by a tunnel amplitude $t_{a,\alpha} = t_{\alpha,a}$ and layers b and β are connected by a tunnel amplitude $t_{b,\beta} = t_{\beta,b}$. We use the notation $t = t_{a,\alpha} = t_{b,\beta}$ and denote by t_0 the tunnel amplitude within each layer (see Eqs. (3, 4)).

The definition of the tunnel Hamiltonian that we use for the F/S/F trilayer is slightly different from the conventional definition given by (4):

$$\mathcal{W}_{\mathrm{FSF}} = \frac{t}{\sqrt{2}} \sum_{\mathbf{x},\sigma} \left(c^+_{x,y,\alpha,\sigma}c_{x,y,a,\sigma} + c^+_{x,y,a,\sigma}c_{x,y,\alpha,\sigma}\right) + \frac{t}{\sqrt{2}} \sum_{\mathbf{x},\sigma} \left(c^+_{x,y,\beta,\sigma}c_{x,y,b,\sigma} + c^+_{x,y,b,\sigma}c_{x,y,\beta,\sigma}\right). \tag{12}$$

With the factors $\sqrt{2}$ the F/S/F trilayer with $L_S/a_0 = 1$ in the parallel alignment is equivalent to the F/S bilayer with $L_S/a_0 = 1$ and a tunnel amplitude equal to t. The correspondence between the bi and trilayer is useful for checking the numerical simulations. For $L_S/a_0 \geq 2$ we carry out the simulations of the F/S/F trilayer but we note that in the parallel alignment the qualitative predictions are valid also for F/S bilayers as long as the thickness of the superconductor is smaller than the coherence length.

We note $\hat{K}_{\alpha,\alpha} = \hat{h}_{\alpha,\alpha}\hat{t}_{\alpha,a}\hat{h}_{a,a}\hat{t}_{a,\alpha}$, $\hat{K}_{\beta,\beta} = \hat{h}_{\beta,\beta}\hat{t}_{\beta,b}\hat{h}_{b,b}\hat{t}_{b,\beta}$, $\hat{K}_{\alpha,\beta} = \hat{h}_{\alpha,\beta}\hat{t}_{\beta,b}\hat{h}_{b,b}\hat{t}_{b,\beta}$, $\hat{K}_{\beta,\alpha} = \hat{h}_{\beta,\alpha}\hat{t}_{\alpha,a}\hat{h}_{a,a}\hat{t}_{a,\alpha}$. The Green's function $\hat{G}_{\alpha,\alpha}$ is given by

$$\hat{G}_{\alpha,\alpha} = \left[\hat{I} - \hat{K}_{\alpha,\alpha} - \hat{K}_{\alpha,\beta}\left[\hat{I} - \hat{K}_{\beta,\beta}\right]^{-1}\hat{K}_{\beta,\alpha}\right]^{-1} \times \left[\hat{h}_{\alpha,\alpha} + \hat{K}_{\alpha,\beta}\left[\hat{I} - \hat{K}_{\beta,\beta}\right]^{-1}\hat{h}_{\beta,\alpha}\right], \tag{13}$$

and $\hat{G}_{\beta,\alpha}$ is given by

$$\hat{G}_{\beta,\alpha} = \left[\hat{I} - \hat{K}_{\beta,\beta}\right]^{-1}\left[\hat{h}_{\beta,\alpha} + \hat{K}_{\beta,\alpha}\hat{G}_{\alpha,\alpha}\right]. \tag{14}$$

The Green's function $\hat{G}_{\alpha,\beta}$ is deduced from $\hat{G}_{\beta,\alpha}$ through the relation $\hat{G}^{\tau_1,\tau_2}_{\alpha,\beta} = \hat{G}^{\tau_2,\tau_1}_{\beta,\alpha}$, where τ_1 and τ_2 are the Nambu indexes. $\hat{G}_{\beta,\beta}$ is given by

$$\hat{G}_{\beta,\beta} = \left[\hat{I} - \hat{K}_{\beta,\beta}\right]^{-1}\left[\hat{h}_{\beta,\beta} + \hat{K}_{\beta,\alpha}\hat{G}_{\alpha,\beta}\right]. \tag{15}$$

We deduce the values of $\hat{G}_{a,a}$, $\hat{G}_{b,b}$, $\hat{G}_{a,b}$ and $\hat{G}_{b,a}$ as well as $G_{i,i}$ in the superconductor:

$$\hat{G}_{i,i} = \hat{h}_{i,i} + \hat{h}_{i,\alpha}\hat{t}_{\alpha,a}\hat{G}_{a,a}\hat{t}_{a,\alpha}\hat{h}_{\alpha,i} + \hat{h}_{i,\alpha}\hat{t}_{\alpha,a}\hat{G}_{a,b}\hat{t}_{b,\beta}\hat{h}_{\beta,i} + \hat{h}_{i,\beta}\hat{t}_{\beta,b}\hat{G}_{b,a}\hat{t}_{a,\alpha}\hat{h}_{\alpha,i} + \hat{h}_{i,\beta}\hat{t}_{\beta,b}\hat{G}_{b,b}\hat{t}_{b,\beta}\hat{h}_{\beta,i}. \tag{16}$$

To obtain the pair amplitude in the ferromagnets and superconductor we first calculate recursively the $\hat{h}$'s and next evaluate $\hat{G}_{1,2}$. The evaluation of the self-consistent superconducting gap is done either by dichotomy if $L_S/a_0 = 1, 2$ or by iterations of the self-consistency equation (9) if $L_S/a_0 \geq 3$.

4 F/S/F trilayers with $L_S, L_F \ll \xi_S^{(\perp)}, \xi_F^{(\perp)}$

In this section we consider the regime $L_S, L_F \ll \xi_S^{(\perp)}, \xi_F^{(\perp)}$, establish a connection between the LDOS and the self-consistent superconducting gap, and show that the regime $h_{\rm ex}/\Delta_0 \sim 1$ is characterized by Andreev bound states competing with the formation of a minigap.

4.1 Self-consistent superconducting gap for weak ferromagnets in the parallel alignment

4.1.1 Role of the thicknesses of the electrodes

We have shown in Figure 3 the temperature dependence of the superconducting gap for values of (L_S, L_F) such that $L_S, L_F \ll \xi_S^{(\perp)}, \xi_F^{(\perp)}$. We used $L_S/a_0 = 1$ in Figure 3 but similar results were obtained with $L_S/a_0 = 2$. As expected from Appendix A the breakdown of superconductivity in the resonant F/S/F trilayer in the parallel alignment resembles the case $(L_S/a_0, L_F/a_0) = (1,1)$ [40]: as temperature is reduced the superconducting gap increases, reaches a maximum and decreases to zero. We obtain a reentrant behavior in a narrow range of interface transparencies (not shown in Fig. 3). By contrast we obtain a monotonic behavior for off-resonant values of $(L_S/a_0, L_F/a_0)$, as expected from Appendix A.

The values of the tunnel amplitude needed to destroy superconductivity for off-resonant trilayers (see Figs. 3b and d) is almost ten times larger than in the resonant case (see Figs. 3a and c). This is because the effective coupling between the superconductor and ferromagnets is much weaker in the off-resonant case due to the differences in the density of states.

4.1.2 Role of the exchange field

We repeated the simulations for the F/S/F trilayer with $(L_S/a_0, L_F/a_0) = (2,2)$ but with different values of $h_{\rm ex}/\Delta_0$. For the smallest value of $h_{\rm ex}/\Delta_0$ ($h_{\rm ex}/\Delta_0 = 0.28$) we obtained a monotonic decrease of the superconducting gap as a function of temperature for all values of the tunnel amplitude. For $h_{\rm ex}/\Delta_0 = 0.56, 0.83, 1.11, 1.39$ we obtained a non monotonic temperature dependence of the superconducting gap similar to Figures 3a and 3b. The non monotonic variation of the superconducting gap occurs typically for $h_{\rm ex}$ being a fraction of Δ_0 up to values slightly above Δ_0.

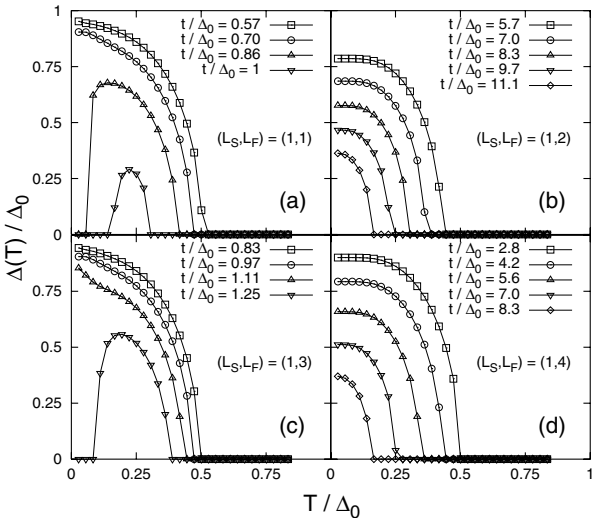

Fig. 3. Temperature dependence of the self-consistent superconducting gap for the F/S/F trilayer in the parallel alignment with $(L_S/a_0, L_F/a_0) = (1,1)$ (a), $(1,2)$ (b), $(1,3)$ (c), $(1,4)$ (d), with weak ferromagnets ($h_{\rm ex}/\Delta_0 = 0.83$). L_F and L_S are small compared to $\xi_{S,0}^{(\perp)} = 2t_0a_0/\pi\Delta_0 = 17.7a_0$, $\xi_F^{(\perp)} = 2t_0a_0/\pi h_{\rm ex} = 21.2a_0$ and $\lambda_F = 6.28a_0$. We use $\Delta_0/\epsilon_F = 0.014$ and $t_0/\epsilon_F = 0.4$.

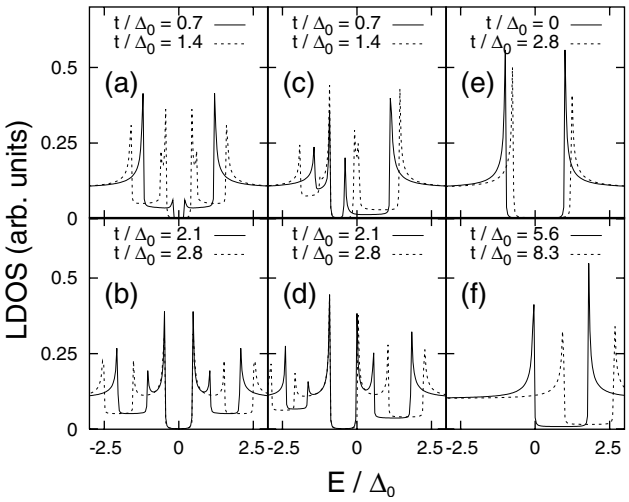

Fig. 4. Energy dependence of the spin-up LDOS (in arbitrary units) in the superconducting layer of the F/S/F trilayer in the parallel alignment with $(L_S/a_0, L_F/a_0) = (1,3)$. The superconducting gap, equal to Δ_0, is not self-consistent. (a) and (b) correspond to $h_{\rm ex}/\Delta_0 = 0$, $\xi_F^{(\perp)} = \infty$ (N/S interface). (c) and (d) correspond to $h_{\rm ex}/\Delta_0 = 0.83$, $\xi_F^{(\perp)} = 21.2a_0$ (F/S interface with weak ferromagnets). (e) and (f) correspond to $h_{\rm ex}/\Delta_0 = 13.9$, $\xi_F^{(\perp)} = 1.3a_0$ (F/S interface with strong ferromagnets). We use $\Delta_0/\epsilon_F = 0.014$. $t_0/\epsilon_F = 0.4$, $\eta/\Delta_0 = 8.3 \times 10^{-3}$, $\lambda_F = 6.28a_0$.

4.2 Relation between the local density of states and the self-consistent superconducting gap

4.2.1 Local density of states in the parallel alignment

The spin-up LDOS $\rho_\uparrow(\omega)$ in the superconductor is shown in Figure 4 for the F/S/F trilayer in the parallel alignment, for $(L_S/a_0, L_F/a_0) = (1,3)$. We obtained similar results for $(L_S/a_0, L_F/a_0) = (2,2)$. The spin-down LDOS $\rho_\downarrow(\omega)$ is obtained through the relation $\rho_\downarrow(\omega) = \rho_\uparrow(-\omega)$. The zero temperature superconducting gap Δ is fixed to the BCS value Δ_0 of an isolated superconducting layer.

The case of a N/S interface is shown in Figures 4a and 4b. The LDOS is symmetric with respect to a change of sign in energy, as expected in the absence of an

exchange field. There exists a minigap at the Fermi energy so that superconductivity is robust against increasing the tunnel amplitude t. Increasing t gives rise to pairs of Andreev bound states at opposite energies (see Fig. 4a). Each peak corresponds to a miniband, which is visible in Figure 4b obtained with larger values of t. The formation of the minibands is related to the infinite planar geometry: the layers are infinite in the x and y directions (see Fig. 1) and there is thus a degeneracy associated to the position of the Andreev bound state in the (x, y) plane. The bound state can delocalize in the (x, y) plane and thus acquire a dispersion which would not occur if the dimensions H and D (see Fig. 1) were small compared to the BCS coherence length, a situation considered in reference [28].

For weak ferromagnets with t, $h_{\rm ex}$ and Δ having the same order of magnitude (panel (c) in Fig. 4) we obtain one Andreev bound state miniband inside the gap and one resonant scattering state above the gap. The Andreev bound state miniband moves to the Fermi energy as the tunnel amplitude t increases (see Fig. 4c) and appears at a positive energy for larger values of t (see Fig. 4d).

For larger values of the exchange field the Andreev bound state miniband disappears from the LDOS. For $h_{\rm ex}/\Delta_0 \gg 1$ the induced exchange field is opposite to the magnetization in the ferromagnets [35,36].

There are thus two qualitatively different depairing mechanisms for strong and weak ferromagnets. For strong ferromagnets with $h_{\rm ex}/\Delta_0 \gg 1$ (see Figs. 4e and 4f) the breakdown of superconductivity is due mainly to Zeeman splitting. The case of very weak ferromagnets ($h_{\rm ex}/\Delta_0 \ll 1$) resembles that case $h_{\rm ex}/\Delta_0 = 0$: non perturbative Andreev bound states are generated in the superconducting gap approximately at opposite energies. In the case $h_{\rm ex}/\Delta_0 \sim 1$ the Andreev bound state miniband can be at zero energy, therefore destructing the minigap.

4.2.2 Finite temperature local density of states

The spin-up LDOS at a finite temperature T is related the conductance of a scanning tunneling microscope (STM) in which the tip is made of a half-metal ferromagnet. The finite temperature current at an arbitrary voltage is obtained through Keldysh formalism. The finite temperature LDOS is found to be

$$\rho_T(\omega) = \int d\omega' \frac{\rho(\omega')}{4T\cosh^2\left(\frac{\omega'-\omega}{2T}\right)}, \qquad (17)$$

where $\rho(\omega)$ is equal to the zero temperature LDOS.

We calculated the finite temperature LDOS of the $(L_S/a_0, L_F/a_0) = (1, 3)$ trilayer in the parallel alignment (see Fig. 5). Increasing temperature tends to reduce the intensity of the Andreev bound state at the Fermi energy in Figure 4c so that the LDOS at the Fermi energy decreases if T increases. For relatively large values of T the peak structure has almost disappeared from the LDOS but there remains a minimum associated to the superconducting gap that is significantly filled. As T increases there is thus a first cross-over where the peak at the Fermi energy disappears and a superconducting minigap is restored, and a second cross-over where the superconducting gap disappears. The first cross over occurs at a temperature equal to the bandwidth of the Andreev bound state miniband and the second cross-over occurs at a temperature comparable to the zero temperature superconducting gap. The finite temperature LDOS is thus in a qualitative agreement with the non monotonic self-consistent superconducting gap.

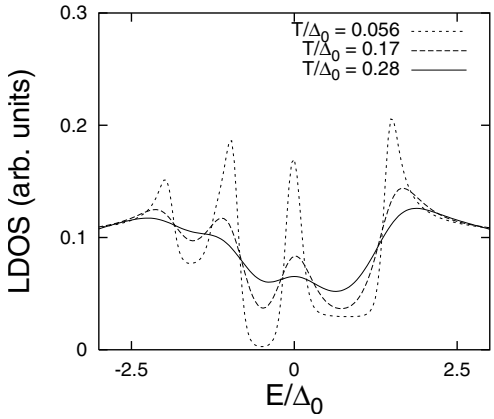

Fig. 5. Energy dependence of the finite temperature spin-up LDOS (in arbitrary units) in the superconducting layer of the F/S/F trilayer in the parallel alignment with $(L_S/a_0, L_F/a_0) = (1, 3)$. The zero temperature LDOS corresponds to Figure 4c with $t/\Delta_0 = 1.4$.

Reentrance obtained in a narrow range of interface transparencies [40] can also be explained by this qualitative picture: if the Andreev bound state miniband is narrow and located at a slightly positive energy like in Figure 4c then the LDOS at the Fermi energy is vanishingly small at $T = 0$ since the Fermi energy is not in the Andreev bound state miniband. By increasing T the width of the Andreev bound state miniband increases so that the density of states at the Fermi energy increases. By further increasing T the intensity of the Andreev bound state miniband is reduced, and the density of states at the Fermi energy decreases. This behavior is compatible with a reentrant behavior of the self-consistent superconducting gap. The correlation between the low temperature superconducting gap and the LDOS at the Fermi energy is further established in Section 6.

4.2.3 Local density of states in the parallel alignment

The spin-up LDOS in the antiparallel alignment is shown in Figure 6. The LDOS is symmetric with respect to a change of sign of energy, but not equivalent to the LDOS of a N/S interface (see Figs. 4a and 4b). There exists a well-defined minimum at the Fermi energy corresponding to the superconducting minigap. The energy dependence of the LDOS in the antiparallel alignment shows that superconductivity is stronger than in the parallel alignment, both for weak and strong ferromagnets. This is expected because of the exchange field induced in the superconductor in the antiparallel alignment is reduced compared to

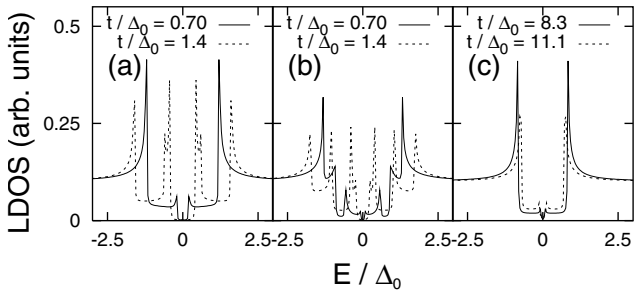

Fig. 6. Energy dependence of the spin-up LDOS (in arbitrary units) in the superconducting layer of the F/S/F trilayer in the antiparallel alignment with $(L_S/a_0, L_F/a_0) = (1, 3)$. The superconducting gap, equal to Δ_0, is not self-consistent. (a) and (b) correspond to $h_{\rm ex}/\Delta_0 = 0.83$, $\xi_F^{(\perp)} = 21.1a_0$ (weak ferromagnets). (c) corresponds to $h_{\rm ex}/\Delta_0 = 2.78$, $\xi_F^{(\perp)} = 6.4a_0$ (strong ferromagnets). We used $\Delta_0/\epsilon_F = 0.014$, $t_0/\epsilon_F = 0.4$, $\eta/\Delta_0 = 8.3 \times 10^{-3}$ and $\lambda_F = 6.28a_0$.

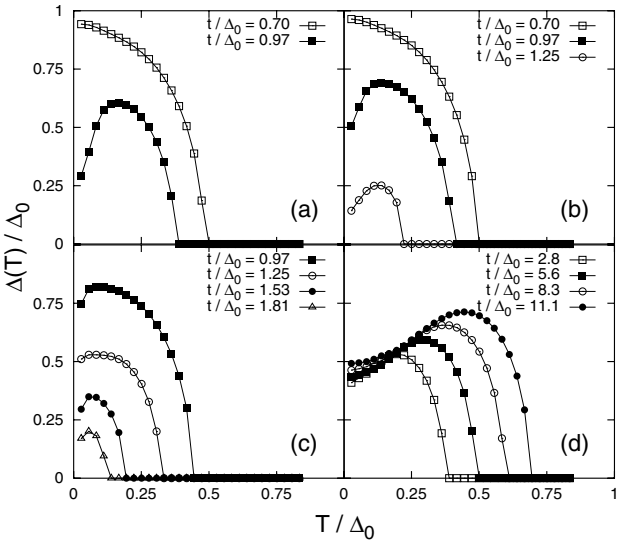

Fig. 7. Temperature dependence of the self-consistent superconducting gap of the F/S/F trilayer in the parallel alignment with $(L_S/a_0, L_F/a_0) = (1, 1)$ in the presence of disorder in the superconducting layer. Without vertex corrections we use $h_{\rm ex}/\Delta_0 = 0.83$, $\delta_S^{(0)} = 6.2$ (a), $\delta_S^{(0)} = 7.6$ (b), $\delta_S^{(0)} = 9.8$ (c). (d) corresponds to $\delta_S^{(0)} = 9.8$ with vertex corrections. In all cases we use $\delta_F^{(0)} = 0$.

the parallel alignment [31]. The self-consistent superconducting gap has a monotonic temperature dependence in this case which is because a well-defined minigap is obtained in the LDOS.

4.3 Role of disorder for weak ferromagnets and for the F/S/F trilayer with atomic thickness

Disorder plays an important role in the proximity effect. Diffusive N/S interfaces are described by quasiclassical theory [54]. A small disorder can be incorporated in our description based on microscopic Green's functions like in reference [53] (see Appendix B). The strength of disorder in the superconductor is characterized by $\delta_S^{(0)} = \sqrt{n_\alpha u_\alpha^2}/\Delta_0$, where n_α is the concentration of impurities and u_α is the scattering potential, and we use a similar parameter $\delta_F^{(0)}$ to characterize disorder in the ferromagnets. We obtain a significant effect of disorder for relatively large values of $\delta_S^{(0)}$ and $\delta_F^{(0)}$.

4.3.1 Disorder in the superconducting and ferromagnetic layers

The temperature dependence of the self-consistent superconducting gap in the presence of disorder in the superconductor is shown in Figure 7 for $(L_S/a_0, L_F/a_0) = (1, 1)$ in the parallel alignment. In the absence of disorder Figure 7 corresponds to Figure 3a. The effect of disorder is to reduce the effect of the tunnel amplitude [40] so that if disorder increases a larger value of t is needed to destroy superconductivity. Comparing Figures 3 and 7 we see that the variations of $\Delta(T)$ are affected by a weak disorder especially if the F/S/F trilayer in the parallel alignment is close to the breakdown of superconductivity. In this case the dimensionless parameter controlling the strength of disorder is $\delta_S = \delta_S^{(0)}\Delta_0/\Delta(T)$ which can be much larger than $\delta_S^{(0)}$.

4.3.2 Vertex corrections

There exist two perturbative series: one in the hopping amplitude t and the other in the disorder scattering potential u. Vertex corrections arise from diagrams that mix the two series (see Appendix B2). The temperature dependence of the self-consistent superconducting gap with the vertex corrections is shown in Figure 7d. The critical temperature is larger if vertex corrections are included. We obtain a non monotonic temperature dependence of the superconducting gap even in the presence of vertex corrections. The role of vertex corrections increases if t increases since the vertex correction term is proportional to $n_\alpha t^2 u_\alpha^2$.

5 Finite thickness in the superconductor ($L_S \lesssim \xi_S^{(\perp)}$ and $L_F \ll \xi_F^{(\perp)}$)

In this section we include a finite thickness in the superconductor for $L_F \ll \xi_F^{(\perp)}$. For weak ferromagnets in the regime $h_{\rm ex}/\Delta_0 \sim 1$ we obtain non monotonic temperature dependences of the self-consistent superconducting gap in the parallel alignment, therefore confirming Section 4.

We have shown in Figure 8a the variation of the self-consistent superconducting gap in the middle of the superconductor as a function of the reduced exchange field $h_{\rm ex}/\Delta_0$. As expected from the variation of the critical temperature [38,47,48] we obtain a minimum if the exchange field is comparable to the superconducting gap. Moreover we obtain a minimum also in the antiparallel alignment that is related to the minigap formed in between Andreev bound states at opposite energies (see Sect. 4.2.3).

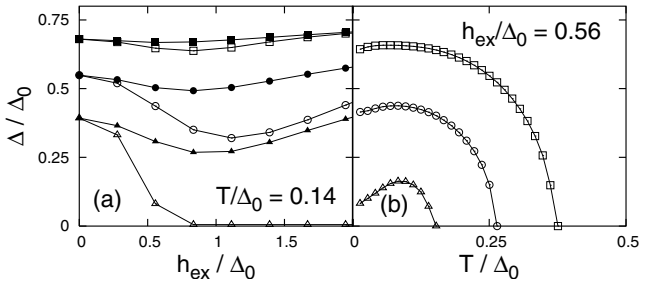

Fig. 8. (a) Variation of the self-consistent superconducting gap calculated at $T/\Delta_0 = 0.14$ in the parallel (P) alignment (open symbols) and in the antiparallel (AP) alignment (filled symbols) as a function of h_{ex}/Δ_0. (b) Variation of the self-consistent superconducting gap calculated with $h_{ex}/\Delta_0 = 0.56$ in the parallel alignment, as a function of T/Δ_0. We used in both cases $(L_F/a_0, L_S/a_0) = (11, 11)$. The Fermi wave length is $\lambda_F = 6.28a_0$. We use $t/\Delta_0 = 5.6$ (□ in the P alignment and ■ in the AP alignment), $t/\Delta_0 = 8.3$ (○ in the P alignment and • in the AP alignment), and $t/\Delta_0 = 11.1$ (△ in the P alignment and ▲ in the AP alignment).

The full temperature dependence of the self-consistent superconducting gap in the parallel alignment is shown in Figure 8b for $L_S/a_0 = 11$ (comparable to $\xi_S^{(\perp)}/a_0$). We obtain a maximum in the variation of $\Delta(T)/\Delta_0$ in the parallel alignment. We carried out the same simulation in the antiparallel alignment and found a monotonic temperature dependence of the self-consistent superconducting gap (not shown in Fig. 8).

6 Finite thickness in the ferromagnets ($L_S \ll \xi_S^{(\perp)}$ and $L_F \gtrsim \xi_F^{(\perp)}$)

We discuss now the regime $L_S \ll \xi_S^{(\perp)}$ and $L_F \gtrsim \xi_F^{(\perp)}$. We find Andreev bound states at the Fermi energy in the parallel alignment for strong ferromagnets, correlated with non monotonic temperature dependences of the self-consistent superconducting gap.

The regime $L_F \gtrsim \xi_F$ is characterized by oscillations of the self-consistent superconducting gap, critical temperature and pair amplitude as a function of L_F. We obtain bound states within the superconducting gap and resonant scattering states outside the superconducting gap. We calculated systematically the LDOS and the self-consistent superconducting gap for $L_S/a_0 = 1, 2$ and $L_F/a_0 = 1, ..., 100$, in the parallel and antiparallel alignments (see Fig. 9). The systematic calculation of the finite temperature LDOS given by equation (17) is too demanding from a computational point of view. Instead we calculate the LDOS at zero temperature with $\eta = T$. The consistency between the two calculations was verified in a few cases. Depending on the interface transparencies $\Delta(L_F/a_0)/\Delta_0$ tends either to a finite value or to zero in the limit $L_F/a_0 \to +\infty$. We concentrate on the first case only. For $1 \leq L_F/a_0 \leq 40$ we see in Figure 9 that on average the superconducting gap is smaller when the LDOS at the Fermi energy is larger. For $L_S/a_0 = 1$ and

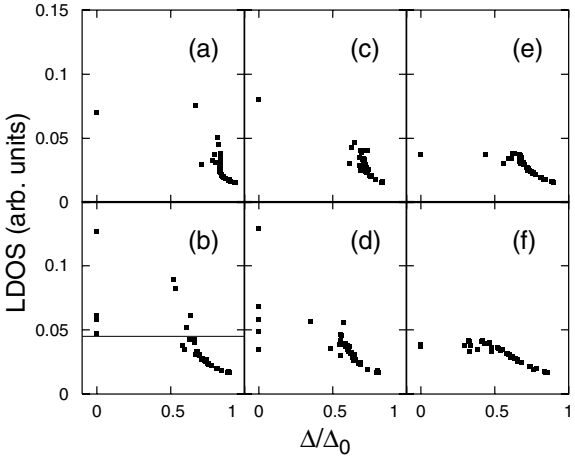

Fig. 9. Correlation between Δ/Δ_0 and the LDOS at the Fermi energy (in arbitrary units) for $L_S/a0 = 1$ and L_F/a_0 between 1 and 40. The temperature is $T/\Delta_0 = 0.14$. In the calculation of the LDOS the superconducting gap is not self-consistent. We use strong ferromagnets with $h_{ex}/\Delta_0 = 13.9$ and $\xi_F^{(\perp)} = 1.3a_0$. We use $L_S/a_0 = 1$ and $t/\Delta_0 = 2.1$ (a); $L_S/a_0 = 1$ and $t/\Delta_0 = 2.8$ (b); $L_S/a_0 = 2$ and $t/\Delta_0 = 3.5$ (c); $L_S/a_0 = 2$ and $t/\Delta_0 = 4.2$ (d); $L_S/a_0 = 1$ and $t/\Delta_0 = 2.8$ (e); $L_S/a_0 = 1$ and $t/\Delta_0 = 3.3$ (f). (a), (b), (c), (d) correspond to the parallel alignment. (e) and (f) correspond to the antiparallel alignment. The solid line in (b) corresponds to $\rho(\omega = 0) = 0.045$ (see text).

$t/\Delta_0 = 2.8$ (see Fig. 9b) we obtain $\Delta(T)/\Delta_0 = 0$ for four values of L_F/a_0 ($L_F/a_0 = 4, 6, 11, 13$). For three other values of L_F/a_0 ($L_F/a_0 = 16, 23, 25$) we obtain a non monotonic variation of $\Delta(T)/\Delta_0$. For two other values of L_F/a_0 ($L_F/a_0 = 32$ and $L_F/a_0 = 35$) $\Delta(T)/\Delta_0$ is monotonic but far from the BCS variation. These nine values of L_F/a_0 with an anomalous temperature dependence of the self-consistent superconducting gap have large values of the LDOS at the Fermi energy ($\rho(\omega = 0) > 0.045$ in Figure 9b, in arbitrary units). Like in Section 4.2.1 Andreev bound states near the Fermi energy correlate with unconventional temperature dependences of the superconducting gap.

For $40 \leq L_F/a_0 \leq 100$ corresponding to $L_F \gg \xi_F^{(\perp)}$, we obtain a cloud of points with a small dispersion and with no correlation between the superconducting gap and the LDOS at the Fermi energy. This corresponds to the cross-over to the F/S/F trilayer with bulk ferromagnets.

We obtain bound states within the superconducting gap and unconventional temperature dependences of the superconducting gap with strong ferromagnets in the parallel alignment. By contrast with strong ferromagnets we obtain a conventional temperature dependence of the superconducting gap for the F/S/F trilayer with smaller values of $(L_S/a_0, L_F/a_0)$ [40].

We carried out the same simulation in the antiparallel alignment and found that $\Delta(T)/\Delta_0$ is close to the BCS temperature dependence of the superconducting gap for all values of L_S/a_0 between 1 and 100. A larger density of states at the Fermi energy correlates with smaller values of

the self-consistent superconducting gap like in the parallel alignment (see Figs. 9e and f). Because of the minigap that can be formed since the bound states are at opposite energies (see Fig. 6) we do not obtain the points with large values of the density of states at the Fermi energy like in the parallel alignment. The absence of large values of the LDOS at the Fermi energy is related to the fact that the Andreev levels in the antiparallel alignment do not cross the Fermi energy as the interface transparency is increased.

7 Comparison with other models

The discussion in the preceding sections was restricted to the infinite planar geometry. Now we discuss Andreev bound states in other geometries without imposing self-consistency on the superconducting gap. In Section 7.1 we improve the discussion of a model proposed by recently Vecino et al. [28] in which a ferromagnetic chain is connected to a superconductor [55]. In Section 7.2 we compare the LDOS to a model discussed recently by Cserti et al. [29].

7.1 A one dimensional model

We suppose that the superconductor and ferromagnets are described by 1D chains with open boundary conditions with L_S/a_0 sites in the superconductor and L_F/a_0 sites in the ferromagnet. We denote by t_S (t_F) the hopping amplitude in the superconductor (ferromagnet) and we use $t_S = t_F$. The energy level spacing in the superconductor is much smaller than the superconducting gap Δ.

We have shown in Figure 10 the evolution of the energy of Andreev bound states as a function of the length of the ferromagnetic chain obtained with the algorithm presented in Appendix C. The spectrum is symmetric under a change of sign in energy if we keep all energy levels into account. Andreev bound states arising from the gap edges move to the Fermi energy as L_F/a_0 increases [28]. There is level repulsion between Andreev bound state and oscillations of the energy levels with a period of order 10 times $\xi_F = 2t_F a_0/\pi h_{\rm ex}$. These oscillations do not exist in reference [28]. Among all Andreev bound states obtained at a fixed L_F/a_0 some have a spectral weight much larger than the other. We keep only the levels having a spectral weight larger than a given cut-off. The evolution of the remaining Andreev bound states as a function of L_F/a_0 is then in agreement with reference [28].

In connection with the discussion in Section 4.2.1 we see that Andreev bound states near the Fermi energy occur only if the ferromagnetic chain is long enough, larger than approximately 10 times $\xi_S = 2t_S a_0/\pi\Delta$. This should be contrasted with the LDOS in the infinite planar limit discussed in Section 4.2.1, and with the model discussed in Section 7.2.

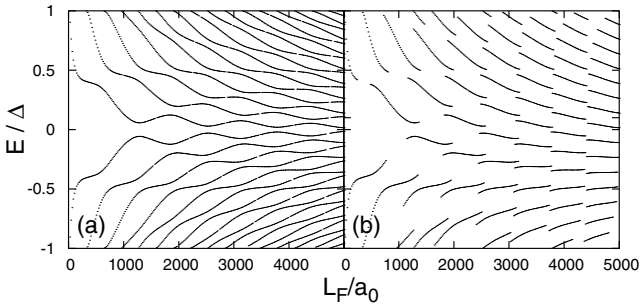

Fig. 10. Reduced energy E/Δ of the Andreev bound states as a function of the number of sites L_F/a_0 in the ferromagnetic chain for weak ferromagnets ($h_{\rm ex}/\Delta = 0.5$). We used the parameters $\Delta/t = \Delta_0/t_F = 0.01$, $t/t_S = 0.01$, $L_S = 10^5 a_0$. The entire spectrum is kept in (a). Only the levels with a residue larger than 2 are kept in (b). The superconducting gap is not self-consistent.

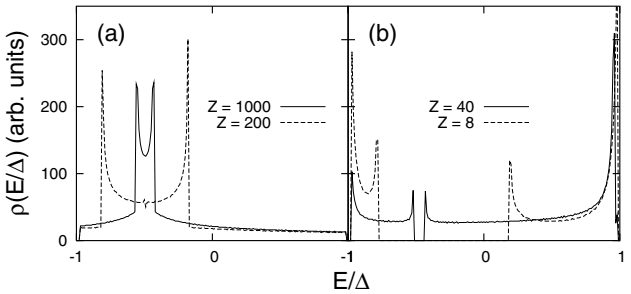

Fig. 11. Density of Andreev bound states (in arbitrary units) $\rho(E/\Delta)$ as a function of reduced energy E/Δ for $Z = 1000$ and $Z = 200$ (a); $Z = 40$ and $Z = 8$ (b). We used the parameters $\Delta/\epsilon_F = 0.02$, $\Delta = 0.01$, $h_{\rm ex}/\Delta = 0.5$, $d = \lambda_F/2$, $W \simeq 15900\lambda_F$ where $\lambda_F = 2\pi/k_F$ is the Fermi wave length.

7.2 Bogoliubov-de Gennes equations

We consider now the model proposed by Cserti et al. [29] in which a 2D ferromagnetic dot with a rectangular shape of dimensions (d, W) is connected to a superconductor (see Fig. 1b). The superconductor has a width W but is infinite in the other direction ($d' = +\infty$ in Fig. 1). Using the solution of this model [29] based on Bogoliubov-de Gennes equations we generated the set $\{E_n\}$ of Andreev bound state energies. Like for the de Gennes-Saint James model [26] the density of bound states is not equal to the LDOS in the superconductor [28]. The evolution of the density of Andreev bound states as a function of the interface transparency is shown in Figure 11. The interface transparency is parametrized by the dimensionless coefficient Z, equal to the repulsive interface potential in units of the Fermi energy [56]. For large values of Z (corresponding to tunnel interfaces) we obtain an Andreev bound state miniband around $E/\Delta_0 = h_{\rm ex}/\Delta_0$. As the interface transparency decreases the miniband broadens and splits into two separate minibands (see Fig. 11). This is in a qualitative agreement with Section 4.2.1 (see Figs. 4c and 4d) where we obtain also Andreev bound state minibands that evolve inside the superconducting gap and can generate a

large density of states at the Fermi energy for some values of the interface transparencies.

8 Conclusions

We have presented a detailed analysis of F/S/F trilayers with weak ferromagnets based on microscopic Green's functions. The exchange field induced in the superconductor in the regime $h_{\rm ex}/\Delta_0 \gg 1$ generates Zeeman splitting of the LDOS while the regime $h_{\rm ex}/\Delta_0 \ll 1$ is characterized by Andreev bound states. In the non perturbative regime $t/\Delta_0 \sim h_{\rm ex}/\Delta_0 \sim 1$ the Andreev bound state miniband crosses the Fermi energy as the interface transparency is increased therefore competing with the formation of a minigap, which explains why the self-consistent superconducting gap is weakened by the formation of an Andreev bound state miniband near the Fermi energy. Increasing temperature decreases the intensity of the Andreev bound state peak in the LDOS which correlates with a reduction of the low temperature self-consistent superconducting gap.

We found non monotonic temperature dependences of the superconducting gap with weak ferromagnets for $L_F, L_S \ll \xi_F^{(\perp)}, \xi_S^{(\perp)}$ as well as for $L_S \sim \xi_S^{(\perp)}$ and $L_F \ll \xi_F^{(\perp)}$. In the regime $L_S \ll \xi_S^{(\perp)}$ and $L_F \gtrsim \xi_F^{(\perp)}$ we obtain non monotonic temperature dependences for some values of L_F/a_0 for strong ferromagnets.

For the F/S/F trilayer in the parallel alignment we find pairs of Andreev bound states at opposite energies but there exists a minigap so that the self-consistent superconducting gap decreases monotonically with temperature. However at a fixed temperature the self-consistent superconducting gap is non monotonic as a function of the exchange field which is due to pairs of Andreev bound states at opposite energies in the regime $h_{\rm ex}/\Delta_0 \sim 1 \ll t/\Delta_0$.

Concerning the induced exchange field in the F/S/F trilayer in the parallel alignment we find that for weak ferromagnets the exchange field is in the same direction as in the ferromagnetic electrodes whereas it is in the opposite direction for strong ferromagnets.

The author wishes to thank D. Feinberg for fruitful discussions and useful comments on the manuscript.

Appendix A: Resonances in lateral confinement

In this appendix we account for the differences between the resonant and off-resonant F/S/F trilayers. The wave function in the lateral direction within a given electrode is described by the tight binding Hamiltonian

$$\mathcal{H} = t_0 \sum_z \left[|z+1\rangle\langle z| + |z\rangle\langle z+1| \right], \qquad \text{(A.1)}$$

where t_0 is the hopping between neighboring layers, and z/a_0 is an integer between 0 to $L/a_0 - 1$. The eigenstates with open boundary conditions are given by

$$|\psi_n\rangle = \sqrt{\frac{2a_0}{L+a_0}} \sum_{z=0}^{L/a_0-1} \sin\left(n\pi \frac{z+a_0}{L+a_0}\right)|z\rangle, \qquad \text{(A.2)}$$

and the energy is given by

$$\epsilon_n(L) = 2t_\perp \cos\left(\frac{n\pi a_0}{L+a_0}\right), \qquad \text{(A.3)}$$

with $n = 1, ..., L/a_0$. Let us consider a F/S/F trilayer with L_F/a_0 layers in the ferromagnets and L_S/a_0 layers in the superconductor. Quasiparticles in the superconductor with a transverse quantum number n_S can tunnel in the ferromagnets only if there exists an energy level with quantum number n_F close to resonance in the ferromagnets, such that $\epsilon_{n_S}(L_S) \simeq \epsilon_{n_F}(L_F)$. If tunneling between the ferromagnets and superconductor is not resonant then the F/S/F trilayer behaves as if the ferromagnets were insulating. The lowest off-resonant values of $(L_S/a_0, L_F/a_0)$ correspond to $(L_S/a_0, L_F/a_0) = (1,2), (1,4), (2,1), (2,3), (3,2), (3,4), (4,1), (4,2), (4,3)$. The lowest resonant values of $(L_S/a_0, L_F/a_0)$ correspond to $(L_S/a_0, L_F/a_0) = (1,1), (1,3), (2,2), (3,1), (3,3)$.

Appendix B: Disorder in the F/S/F trilayer with atomic thickness

In this appendix we give the Dyson equations of a F/S/F trilayer in the presence of disorder.

B.1 Disorder in the superconducting and ferromagnetic layers

We first neglect vertex corrections that are discussed in Section 4.3.2. We replace the Green's functions $\hat{g}_{\alpha,\alpha}$ of the superconducting layer by the Green's function $\hat{g}^{(d)}_{\alpha,\alpha}$ of the superconducting layer in the presence of disorder. To second order in disorder the Dyson equation takes the form

$$\hat{g}^{(d)}_{\alpha,\alpha}(\mathbf{k},\omega) = \hat{g}_{\alpha,\alpha}(\mathbf{k},\omega) + n_\alpha a_0^2 \hat{g}_{\alpha,\alpha}(\mathbf{k},\omega) \times \int \frac{d\mathbf{k}'}{(2\pi)^2} \overline{\hat{u}_\alpha(\mathbf{k}-\mathbf{k}')\hat{g}_{\alpha,\alpha}(\mathbf{k}',\omega)\hat{u}_\alpha(\mathbf{k}'-\mathbf{k})}\hat{g}^{(d)}_{\alpha,\alpha}(\mathbf{k},\omega), \qquad \text{(B.1)}$$

where n_α is the concentration of impurities and the overline denotes an averaging over disorder. Equation (B.1) is solved according to

$$\begin{bmatrix} g^{(d),1,1}_{\alpha,\alpha} & f^{(d),1,2}_{\alpha,\alpha} \\ f^{(d),2,1}_{\alpha,\alpha} & g^{(d),2,2}_{\alpha,\alpha} \end{bmatrix} = \frac{1}{\mathcal{D}} \left\{ \begin{bmatrix} g^{1,1}_{\alpha,\alpha} & f^{1,2}_{\alpha,\alpha} \\ f^{2,1}_{\alpha,\alpha} & g^{2,2}_{\alpha,\alpha} \end{bmatrix} - d \begin{bmatrix} \Sigma_g^{2,2} & \Sigma_f \\ \Sigma_f & \Sigma_g^{1,1} \end{bmatrix} \right\}, \qquad \text{(B.2)}$$

where $d = g^{1,1}_{\alpha,\alpha} g^{2,2}_{\alpha,\alpha} - \left(f^{1,2}_{\alpha,\alpha}\right)^2$ and $\mathcal{D} = 1 + 2 f_{\alpha,\alpha}\Sigma_f - g^{1,1}_{\alpha,\alpha}\Sigma^{1,1}_g - g^{2,2}_{\alpha,\alpha}\Sigma^{2,2}_g + d\Sigma_d$, with $\Sigma_d = \Sigma^{1,1}_g \Sigma^{2,2}_g - (\Sigma_f)^2$. The self-energies due to disorder take the form

$$\begin{bmatrix} \Sigma^{1,1}_g & \Sigma^{1,2}_f \\ \Sigma^{1,2}_f & \Sigma^{2,2}_g \end{bmatrix} = \frac{n_\alpha u_\alpha^2 a_0^2}{(2\pi)^2} \int d\mathbf{k} \begin{bmatrix} g^{1,1}_{\alpha,\alpha}(\mathbf{k}) & f^{1,2}_{\alpha,\alpha}(\mathbf{k}) \\ f^{1,2}_{\alpha,\alpha}(\mathbf{k}) & g^{2,2}_{\alpha,\alpha}(\mathbf{k}) \end{bmatrix}, \quad \text{(B.3)}$$

where n_α is the concentration of impurities and u_α is the scattering potential. We suppose that u_α is independent on wave vector.

The fully dressed Green's function of the connected trilayer without vertex corrections is obtained through

$$\hat{G}_{\alpha,\alpha} = \left[\hat{I} - \hat{g}^{(d)}_{\alpha,\alpha}\hat{t}_{\alpha,a}\hat{g}^{(d)}_{a,a}\hat{t}_{a,\alpha} - \hat{g}^{(d)}_{\alpha,\alpha}\hat{t}_{\alpha,b}\hat{g}^{(d)}_{b,b}\hat{t}_{b,\alpha}\right]^{-1} \hat{g}^{(d)}_{\alpha,\alpha}, \quad \text{(B.4)}$$

where $\hat{G}_{\alpha,\alpha}$ stands for $\hat{G}_{\alpha,\alpha}(\mathbf{k},\omega)$, and $\hat{g}^{(d)}_{i,i}$ stands for $\hat{g}^{(d)}_{i,i}(\mathbf{k},\omega)$, with $i = \alpha, a, b$.

B.2 Vertex corrections

Lowest order vertex corrections correspond to processes in which a quasiparticle of the superconducting layer makes an excursion in one of the ferromagnetic layers in between two scatterings on a given impurity in the superconducting layer. The fully dressed Green's function is obtained through

$$\begin{aligned} \hat{G}_{\alpha,\alpha} = {} & \hat{g}^{(d)}_{\alpha,\alpha} \\ & + \hat{g}^{(d)}_{\alpha,\alpha}\hat{t}_{\alpha,a}\hat{g}^{(d)}_{a,a}\hat{t}_{a,\alpha}\hat{G}_{\alpha,\alpha} + \hat{g}^{(d)}_{\alpha,\alpha}\hat{t}_{\alpha,b}\hat{g}^{(d)}_{b,b}\hat{t}_{b,\alpha}\hat{G}_{\alpha,\alpha} \\ & + n_\alpha a_0^2 \hat{g}^{(d)}_{\alpha,\alpha} \int \frac{d\mathbf{k}'}{(2\pi)^2} \overline{\hat{u}_\alpha \hat{g}'^{(d)}_{\alpha,\alpha}\hat{t}_{\alpha,a}\hat{g}'^{(d)}_{a,a}\hat{t}_{a,\alpha}\hat{g}'^{(d)}_{\alpha,\alpha}\hat{u}_\alpha}\hat{G}_{\alpha,\alpha} \\ & + n_\alpha a_0^2 \hat{g}^{(d)}_{\alpha,\alpha} \int \frac{d\mathbf{k}'}{(2\pi)^2} \overline{\hat{u}_\alpha \hat{g}'^{(d)}_{\alpha,\alpha}\hat{t}_{\alpha,b}\hat{g}'^{(d)}_{b,b}\hat{t}_{b,\alpha}\hat{g}'^{(d)}_{\alpha,\alpha}\hat{u}_\alpha}\hat{G}_{\alpha,\alpha}, \end{aligned} \quad \text{(B.5)}$$

where we used the same notation as for equation (B.4) and $g'^{(d)}_{i,i} = g^{(d)}_{i,i}(\mathbf{k}',\omega)$, $\hat{u}_\alpha = \hat{u}_\alpha(\mathbf{k}-\mathbf{k}')$.

Appendix C: Algorithm for the 1D model

In this appendix we detail the algorithm by which we calculate the energies of the Andreev bound states of the 1D model [28]. In the superconductor the spectral representation of the local propagator is obtained by summing equation (6) over all energy levels of the 1D chain with open boundary conditions:

$$\begin{aligned} g^{1,1}_{\alpha,\beta}(\omega) = {} & \frac{2a_0}{L_S + a_0} \sum_{n=1}^{L_S/a_0} \sin\left(n\pi \frac{x_\alpha + a_0}{L_S + a_0}\right) \\ & \times \sin\left(n\pi \frac{x_\beta + a_0}{L_S + a_0}\right) \left[\frac{u_n^2}{\omega - E_n - i\eta} + \frac{v_n^2}{\omega + E_n - i\eta}\right], \end{aligned} \quad \text{(C.1)}$$

where α and β correspond to two sites in the 1D chain at positions x_α and x_β. Similar expressions are obtained for the "22" and "12" components. In the ferromagnet the energy levels are given by $\epsilon_n^{(\sigma)} = \epsilon_n(L_F) - \sigma h_{\rm ex}$, where $\epsilon_n(L)$ is given by equation (A.3). The local Green's function at the extremity of the 1D ferromagnet is given by

$$g^{(\sigma)}_{a,a}(\omega) = \frac{2a_0}{L_F + a_0} \sum_{n=1}^{L_F} \sin^2\left(\frac{n\pi a_0}{L_F + a_0}\right) \frac{1}{\omega - \epsilon_n^{(\sigma)} - i\eta}. \quad \text{(C.2)}$$

We denote by α a site in the superconductor, chosen far from the boundaries. At site α is connected the extremity "a" of the ferromagnetic chain. We note $t = t_{a,\alpha} = t_{\alpha,a}$. The fully dressed Green's function $G^{1,1}_{\alpha,\alpha}$ of spin-up electrons at site α is deduced from the Dyson equations [28,36,37]. The spectral representation of $G^{1,1}_{\alpha,\alpha}$ is obtained by evaluating numerically the position of the individual energy levels ω_n and their spectral weights R_n: $G^{1,1}_{\alpha,\alpha} = \sum_n R_n^{1,1}/(\omega - \omega_n - i\eta)$. In the limit $\eta \to 0$ the LDOS is given by

$$\rho^{1,1}_{\alpha,\alpha}(\omega) = \frac{1}{\pi}{\rm Im}\left[G^{1,1}_{\alpha,\alpha}(\omega)\right] = \sum_n R_n^{1,1}\delta(\omega - \omega_n). \quad \text{(C.3)}$$

The energy levels and spectral weights can be obtained without approximation to an arbitrary precision by using a dichotomy algorithm.

References

1. M. Tinkham, *Introduction to superconductivity* (McGraw-Hill, 1996)
2. P. Tedrow, R. Meservey, Phys. Rev. Lett. **26**, 192 (1971); P. Tedrow, R. Meservey, Phys. Rev. B **7**, 318 (1973); R. Meservey, P. Tedrow, Phys. Rep. **238**, 173 (1994)
3. R.J. Soulen et al., Science **282**, 85 (1998)
4. S.K. Upadhyay, A. Palanisami, R.N. Louie, R.A. Buhrman, Phys. Rev. Lett. **81**, 3247 (1998)
5. M.J.M. de Jong, C.W. Beenakker, Phys. Rev. Lett. **74**, 1657 (1995)
6. V.I. Fal'ko, C.J. Lambert, A.F. Volkov Pis'ma Zh. Éksp. Teor. Fiz. **69**, 497 (1999) [JETP Lett. **69**, 532 (1999)]
7. F.J. Jedema, B.J. van Wees, B.H. Hoving, A.T. Filip, T.M. Klapwijk, Phys. Rev. B **60**, 16549 (1999)
8. W. Belzig, A. Brataas, Yu.V. Nazarov, G.E.W. Bauer, Phys. Rev. B **62**, 9726 (2000)
9. R. Mélin, Europhys. Lett. **51**, 202 (2000)
10. P. Fulde, A. Ferrel, Phys. Rev. **135**, A550 (1964)
11. A. Larkin, Y. Ovchinnikov, Zh. Eksp. Teor. Fiz. **47**, 1136 (1964) [Sov. Phys. JETP **20**, 762 (1965)]
12. M.A. Clogston, Phys. Rev. Lett. **9**, 266 (1962)
13. E.A. Demler, G.B. Arnold, M.R. Beasley, Phys. Rev. B **55**, 15174 (1997)
14. A.I. Buzdin, L.N. Bulaevskii, S.V. Panyukov, Pis'ma Zh. Eksp. Teor. Fiz. **35**, 147 (1982) [JETP Lett. **35**, 178 (1982)]; A. Buzdin, B. Bujicic, M.Yu. Kupriyanov, Zh. Eksp. Teor. Fiz. **101**, 231 (1992) [Sov. Phys. JETP **74**, 124 (1992)]

15. A.I. Buzdin, M.Yu. Kupriyanov, Pis'ma Zh. Eksp. Teor. Fiz. **52**, 1089 (1990) [JETP Lett. **52**, 487 (1990)]; A.I. Buzdin, M.Yu. Kupriyanov, B. Vujicic, Physica C **185-189**, 2025 (1991)
16. Z. Radović, M. Ledvij, L. Dobrosavljević, A.I. Buzdin, J.R. Clem, Phys. Rev. B **44**, 759 (1991)
17. J.S. Jiang, D. Davidović, D.H. Reich, C.L. Chien, Phys. Rev. Lett. **74**, 314 (1995); J.S. Jiang, D. Davidović, D.H. Reich, C.L. Chien, Phys. Rev. B **54**, 6119 (1996); C.L. Chien, J.S. Jiang, J.Q. Xiao, D. Davidović, D.H. Reich, J. Appl. Phys. **81**, 5358 (1997)
18. L.V. Mercaldo, C. Attanasio, C. Coccorese, L. Maritato, S.L. Prischepa, M. Salvato, Phys. Rev. B **53**, 14040 (1996)
19. Th. Mühge, N.N. Garif'yanov, Yu. V. Goryunov, G.G. Khaliullin, L.R. Tagirov, K. Westerholt, I.A. Garifullin, H. Zabel, Phys. Rev. Lett. **77**, 1857 (1996); Th. Muhge, K. Westerholt, H. Zabel, N.N. Garif'yanov, Yu.V. Goryunov, I.A. Garifullin, G.G. Khaliullin, Phys. Rev. B **55**, 8945 (1997)
20. J. Aartz, J.M.E. Geers, E. Brück, A.A. Golubov, R. Coehoorn, Phys. Rev. B **56**, 2779 (1997); L. Lazar, K. Westerholt, H. Zabel, L.R. Tagirov, Yu. V. Goryunov, N.N. Garif'yanov, I.A. Garifullin, Phys. Rev. B **61**, 3711 (2000); M. Schöck, C. Sürgers, H.V. Löhneysen, Eur. Phys. J. B **14**, 1 (2000)
21. M. Zareyan, W. Belzig, Yu.V. Nazarov, Phys. Rev. Lett. **86**, 308 (2001); M. Zareyan, W. Belzig, Yu.V. Nazarov, Phys. Rev. B **65**, 184505 (2002)
22. V.V. Ryazanov, V.A. Oboznov, A.Yu. Rusanov, A.V. Veretennikov, A.A. Golubov, J. Aarts, Phys. Rev. Lett. **86**, 2427 (2001)
23. T. Kontos, M. Aprili, J. Lesueur, X. Grison, Phys. Rev. Lett. **86**, 304 (2001)
24. W. Guichard, M. Aprili, O. Bourgeois, T. Kontos, J. Lesueur, P. Gandit, Phys. Rev. Lett. **90**, 167001 (2003)
25. H. Sellier, C. Baraduc, F. Lefloch, R. Calemczuk, Phys. Rev. B **68**, 054531 (2003)
26. P.G. de Gennes, D. Saint-James, Phys. Lett. **4**, 151 (1963); D. Saint-James, J. Phys. France **25**, 899 (1964)
27. A.F. Andreev, Sov. Phys. JETP **19**, 1228 (1964)
28. E. Vecino, A. Martin-Rodero, A. Levy Yeyati, Phys. Rev. B **64**, 184502 (2001)
29. J. Cserti, J. Koltai, C.J. Lambert, Phys. Rev. B **69**, 092506 (2004)
30. K. Halterman, O.T. Valls, Phys. Rev. B **66**, 224516 (2002)
31. P.G. de Gennes, Phys. Lett. **23**, 10 (1966)
32. G. Deutscher, F. Meunier, Phys. Rev. Lett. **22**, 395 (1969)
33. J.J. Hauser, Phys. Rev. Lett. **23**, 374 (1969)
34. J.Y. Gu, C.-Y. You, J.S. Jiang, J. Pearson, Ya.B. Bazaliy, S.D. Bader, Phys. Rev. Lett. **89**, 267001 (2002)
35. F.S. Bergeret, A.F. Volkov, K.B. Efetov, Phys. Rev. B **69**, 174504 (2004)
36. H. Jirari, R. Mélin, N. Stefanakis, Eur. Phys. J. B **31**, 125 (2003)
37. R. Mélin, J. Phys.: Condens. Matter **13**, 6445 (2001); V. Apinyan, R. Mélin, Eur. Phys. J. B **25**, 373 (2002)
38. I. Baladié, A. Buzdin, Phys. Rev. B **67**, 014523 (2003); I. Baladié, A. Buzdin, N. Ryzhanova, A. Vedyayev, Phys. Rev. B **63**, 054518 (2001); A. Buzdin, A.V. Vedyayev, N. Ryzhanova, Europhys. Lett. **48**, 686 (1999)
39. A. Buzdin, M. Daumens, Europhys. Lett. **64**, 510 (2003)
40. R. Mélin, D. Feinberg, Europhys. Lett. **65**, 96 (2004)
41. G. Deutcher, D. Feinberg, Appl. Phys. Lett. **76**, 487 (2000)
42. G. Falci, D. Feinberg, F.W.J. Hekking, Europhys. Lett. **54**, 255 (20001)
43. R. Mélin, D. Feinberg, Eur. Phys. J. B **26**, 101 (2002)
44. R. Mélin, S. Peysson, Phys. Rev. B **68**, 174515 (2003)
45. C.J. Lambert, J. Phys.: Condens. Matter **3**, 6579 (1991); C.J. Lambert, R. Raimondi, J. Phys.: Condens. Matter **10**, 901 (1998)
46. A.V. Andreev, A.I. Buzdin, R.M. Osgood III, Phys. Rev. B **43**, 10124 (1991)
47. M. Houzet, A. Buzdin, Europhys. Lett. **58**, 596 (2002)
48. Ya.V. Fominov, N.M. Chtchelkatchev, A.A. Golubov, Ois'ma Zh. Eksp. Teor. Fiz. **74**, 101 (2001) [JETP Lett. **74**, 96 (2001)]; Ya.V. Fominov, N.M. Chtchelkatchev, A.A. Golubov, Phys. Rev. B **66**, 014507 (2002)
49. Yu.N. Proshin, M.G. Khusainov, Zh. Eksp. Teor. Fiz. **113**, 1708 (1998), **116**, 1887 (1999) [JETP **86**, 930 (1998); Yu.N. Proshin, M.G. Khusainov, Zh. Eksp. Teor. Fiz. **89**, 1021 (1999)]; M.G. Khusainov, Yu.N. Proshin, Phys. Rev. B **56**, R14283 (1997); Yu.N. Proshin, M.G. Khusainov, Zh. Eksp. Teor. Fiz. **62**, 6832 (2000)
50. F.S. Bergeret, A.F. Volkov, K.B. Efetov, Phys. Rev. Lett. **18**, 4096 (2001)
51. A. Kadigrobov, R.I. Shekhter, M. Jonson, Europhys. Lett. **54**, 394 (2001)
52. N.M. Chtchelkatchev, I. Burmistrov, Phys. Rev. B **68**, 140501 (2003)
53. A.A. Abrikosov, L.P. Gorkov, I.E. Dzyaloshinski, *Methods of quantum field theory in statistical physics* (Dover Publications, Inc, New York, 1963)
54. W. Belzig, C. Bruder, G. Schön, Phys. Rev. B **54**, 9443 (1996)
55. In reference [28] the Green's functions of the ferromagnet are real numbers. The spin-up and spin-down density of states are thus vanishingly small whereas the opposite is expected for a metallic ferromagnet
56. G.E. Blonder, M. Tinkham, T.M. Klapwijk, Phys. Rev. B **25**, 4515 (1982)